Applied Magnetic Resonance (2020) 51:951–960
https://doi.org/10.1007/s00723-020-01233-x

Applied
Magnetic Resonance

ORIGINAL PAPER

Experimental and Theoretical Study of Emodin Interaction with Phospholipid Bilayer and Linoleic Acid

O. Yu. Selyutina[1,2] · P. A. Kononova[1] · N. E. Polyakov[1,2]

Received: 30 June 2020 / Revised: 23 July 2020 / Published online: 3 September 2020

Abstract

^{1}H NMR technique, optical spectrophotometry and molecular dynamics simulations have been applied to study the effect of the lipid composition on emodin interaction with the lipid bilayer. The special attention was paid on the presence of the unsaturated fatty acid linoleic acid in the lipid bilayer. Emodin (1,3,8-trihydroxy-6-methylanthraquinone) is a natural anthraquinone which shows a wide spectrum of biological activity including anticancer, anti-inflammatory, antiviral, antibacterial, neuroprotective and others. It is assumed that the location of emodin in the lipid membrane is important for its biological activity. It was demonstrated that in the presence of linoleic acid, the pKa value of the emodin significantly increases. Molecular dynamics simulations show that these changes can be associated with the interaction of emodin and linoleic acid inside the bilayer. Also, it was shown that the order of deprotonation positions in the POPC bilayer differs from the deprotonation order in aqueous solution.

1 Introduction

Drug–membrane interactions are widely studied nowadays for several reasons. Firstly, a lot of drugs has intracellular targets and they must overcome a membrane barrier to reach this target. On the other hand, lipids participate in the interaction of proteins with the cell barrier and also regulate the distribution and localization of peripheral proteins to membrane domains. Also, changes in the lipid structure are often related to the development of numerous diseases [1]. Emodin (1,3,8-trihydroxy-6-methylanthraquinone, Fig. 1) is a natural anthraquinone contained in some plants including *Rheum palmatum*, *Polygonum cuspidatum* or *Aloe vera*. These herbs are widely used in traditional medicine in different countries [2]. Emodin has

✉ O. Yu. Selyutina
olga.gluschenko@gmail.com

[1] Institute of Chemical Kinetics and Combustion, Institutskaya St., 3, 630090 Novosibirsk, Russia

[2] Institute of Solid State Chemistry and Mechanochemistry, Kutateladze St., 18, 630128 Novosibirsk, Russia

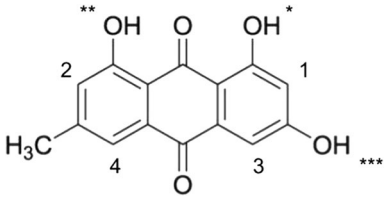

Fig. 1 The chemical structure of emodin

a wide spectrum of biological activities. A number of researches are focused on its anti-inflammatory, anticancer, antiviral, antibacterial, anti-allergic, anti-osteoporotic, anti-diabetic, immunosuppressive, neuroprotective and hepatoprotective activities [2, 3]. The anticancer activity of anthraquinones, including emodin, is related to its association with DNA duplex or with generation of reactive oxygen species, which could damage cell membranes [4].

Membrane-related effects of emodin is the subject of several papers [5, 6]. Because of the its hydrophobicity, emodin interaction with cell membranes may play an important role in its biological activity. It was shown that emodin has an affinity to the lipid membrane and influences the lipid membrane thermotropic behaviour [6]. Also, it was shown that both protonated (EMH) and deprotonated forms (EM-) of the drug are located inside lipid bilayer, though their location slightly differs [5].

Emodin is practically insoluble in water. Phospholipid/water partition coefficient is $(14 \pm 2) \times 10^3$ for neutral emodin in DMPC bilayer [6]. Octanol–water partition coefficient is 3.39 (in logarithmic units).

The lipid composition strongly influences properties of the membrane, such as fluidity, thermotropic behaviour, etc. In particular, it is known that the presence of polyunsaturated fatty acids increases a membrane fluidity [7]. Some unsaturated fatty acids, in particular linoleic acid, could be used in drug delivery [8, 9]. Linoleic acid significantly decreases the phase transition temperature of ethanolamine-containing phospholipids and stabilizes H_{II} structures in phosphatidylethanolamine membranes [10]. Also, some polyunsaturated fatty acids, such as linoleic acid, demonstrate their own anticancer activity [11]. In the present work we have studied an effect of the lipid composition, in particular the effect of linoleic acid, on emodin interaction with the lipid bilayer by means of ^{1}H NMR, optical spectrophotometry and molecular dynamics simulations.

2 Materials and Methods

2.1 Liposome Preparation

Liposomes were formed from 1-palmitoyl-2-oleoylphosphatidylcholine (POPC, Avanti Polar Lipids, purity > 99%) or 1,2-dilinoleoyl-sn-glycero-3-phosphocholine (DLPC, Avanti Polar Lipids, purity > 99%) and linoleic acid (LA, Aladdin, purity > 99%) (Fig. 2). Components were pre-dissolved in chloroform. Emodin was added into chloroform solution. After solvent evaporation, the dry lipid film was hydrated with D_2O.

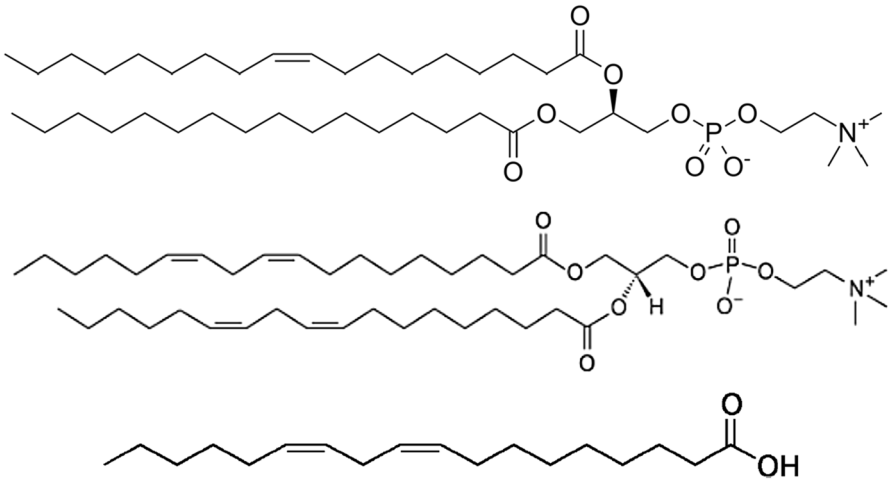

Fig. 2 The chemical structures of POPC (top), DLPC and LA (bottom)

The final concentration of phospholipid in spectrophotometry experiments in NMR experiments—13 mM, of LA—3.5 mM, of emodin—1 mM. The suspension was then sonicated (about 37 kHz, 1 h) to obtain unilamellar liposomes. For optical experiments this suspension was diluted in 6 times. Necessary amounts of HCl and KOH were added to obtain pH dependence of optical and NMR spectra. The absence of the liposome fusion was controlled by the absence in changes of the intensity of signals of a phospholipid [12]. Also, to examine the absence of the liposome fusion, control experiments were done with the addition of shift-reagent $PrCl_3$. Addition of $PrCl_3$ allows to separate the signals of outer and inner $N^+(CH_3)_3$-groups of phospholipid. Conclusions about the presence of unilamellar liposomes in the sample were made by the ratio of signal intensities from outer and inner $N^+(CH_3)_3$-groups of phospholipid.

2.2 Optical Spectrophotometry

Optical spectra of the liposome suspension were measured using SF-2000 (Spectrum, Russia) spectrophotometer in 1-cm quartz cuvette.

2.3 ^{1}H NMR

^{1}H NMR spectra were recorded on Bruker AVHD-500 (500 MHz) NMR spectrometer with temperature control. Deuterated solvent D_2O (99.9% D, Aldrich) was used as received.

2.4 MD Simulations

All simulations were performed using the GROMACS 2018.4 molecular dynamics package [13]. Berger's lipids were used to construct the model pure POPC

bilayer [14]. LA and emodin topology were taken from ATB database [15–17]. SPC water model was employed [18]. Pure bilayer consisted of 128 lipids for simulations at 323 K. Six LA molecules were added into each bilayer using GROMACS gmx mdrun membed option [19]. One emodin molecule was inserted into solvent. Size of model boxes was approximately $6\times6\times8$ nm. Independent runs of 1us duration for each model were calculated with the following model parameters: 2 fs time step, leap-frog integration algorithm, Verlet cut-off scheme [20] with radii of van der Waals and neighbor list equal to 1.2 nm, particle-mesh Ewald method [21] with 4 order cubic interpolation and grid spacing for FFT 0.16. Simulations were performed in an NPT ensemble with temperature $T=323$ K. Temperature and pressure were maintained using Nose–Hoover thermostat [22] and semi-isotropic Parrinello-Rahman barostat [23] (relaxation times were 0.5 and 2 ps respectively).

3 Results

3.1 Optical Spectrophotometry

Figure 3 demonstrates optical absorption spectra of the liposome suspension with emodin in the presence and in the absence of LA. It should be noticed that in the presence of LA the liposome suspension with emodin exhibit a scattering profile which is different for samples with different pH values.

The pH dependence of the POPC suspension with emodin exhibits an isosbestic point (480 nm). For the POPC suspension with emodin in the presence of LA the isosbestic point is not observed, probably, due to different scattering profiles of samples with different pH values.

Figure 4 shows pH dependencies of the optical density at the wavelength 444 nm (absorption maximum) for both samples (in the absence and in the presence of LA).

Values of pKa for both samples were determined by finding the minimum of the derivative of pH dependence. pKa value for POPC + emodine in the absence

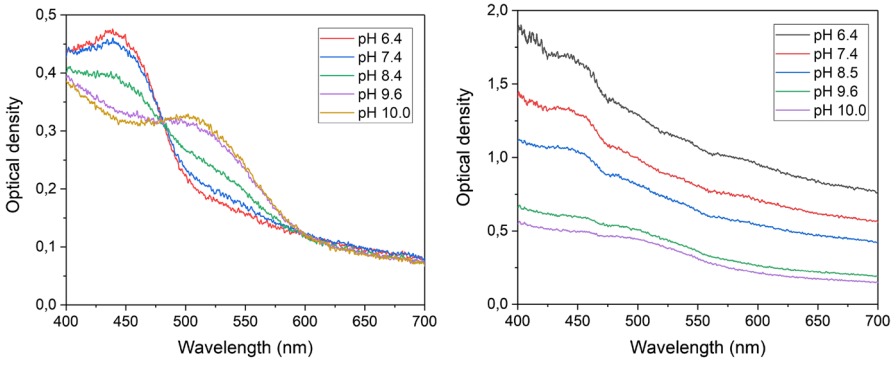

Fig. 3 Optical absorption spectra of POPC + emodin suspension (left) and POPC + LA + emodin suspension (right)

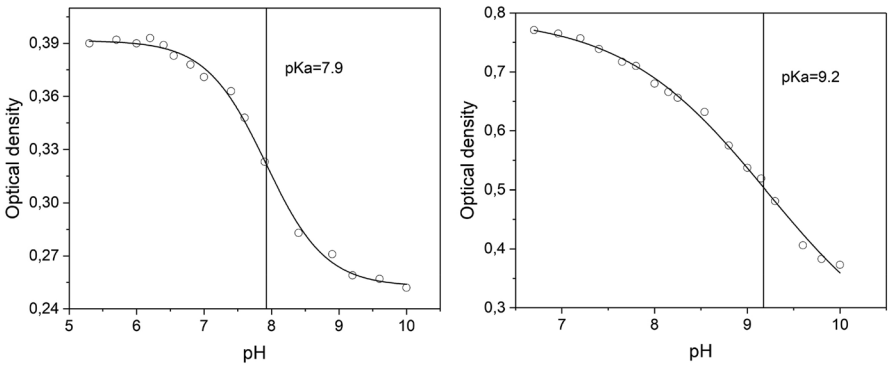

Fig. 4 pH dependencies of the optical density of the POPC + emodin suspension (left) and POPC + LA + emodin suspension (right) at the wavelength 444 nm

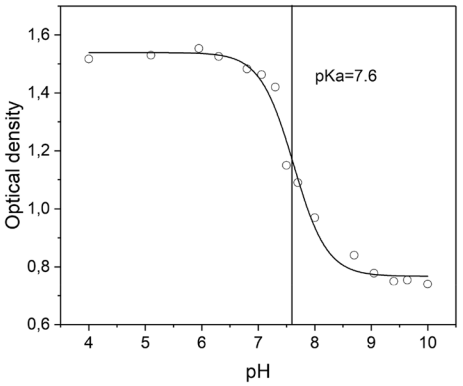

Fig. 5 The pH dependence of the optical density of DLPC + emodin

of LA was 7.9, in the presence of LA—9.2. Also, it should be noticed that in the absence of LA pH dependence is much sharper than in the presence of LA. These experiments were repeated three times, and determined pKa values were 7.9 ± 0.2 in the absence of LA and 9.1 ± 0.2 in the presence of LA.

To understand whether the observed effect is connected with the presence of the unsaturated fatty acid chain, experiments with unsaturated DLPC (Fig. 2) were done. Figure 5 shows the pH dependence of the optical density at the wavelength 444 nm in this sample.

Though this sample also exhibits a strong scattering profile, the pH dependence of the optical density is similar to the sample POPC + emodin without LA. pKa value for this sample is 7.6 ± 0.2 which is also close to pKa of the sample POPC + emodin without LA. It could mean that the observed effect is caused by interaction of emodin with LA inside the lipid membrane.

3.2 ^{1}H NMR

Figure 6 demonstrates fragments of NMR spectra of emodin protons in the POPC suspension in the absence and in the presence of LA.

In both cases shifts of signals to higher magnetic fields are observed while pH increases. In the case of POPC + emodin suspension changes of chemical shift are significantly higher. We observed peak merging for signals 2 and 3 and disappearance of the signal 1 due to overlay with the signal of the water. Changes of chemical shifts are caused by changes of the chemical environment due to deprotonation. Since changes of chemical shift of the proton (1) are higher than other and changes of chemical shift of the proton (2) are the lowest, first deprotonation takes place in position marked by (*) (See Fig. 1). According to [5] in water–methanol mixture first deprotonation takes place in site (***) which exhibits the lowest changes of the chemical shift in our experiments. It could be caused by interaction with the lipid environment.

To check if emodin is in a free form in solution or incorporated inside liposomes ^{1}H NMR spectra of emodin in water and in the suspension of linoleic acid were recorded (Fig. 7). No significant signals of emodin were observed in samples without POPC. It means that all observed chemical shift changes refers to emodin in liposomes.

3.3 MD Simulations

Figure 8 demonstrates density profiles of emodin in the POPC bilayer in the absence and in the presence of LA. Density profiles of N atoms of POPC were calculated to understand the localization of the emodin molecule in the bilayer in both cases. The emodin molecule is localized near polar head groups of POPC in both cases, but its density profile is wider in the presence of LA.

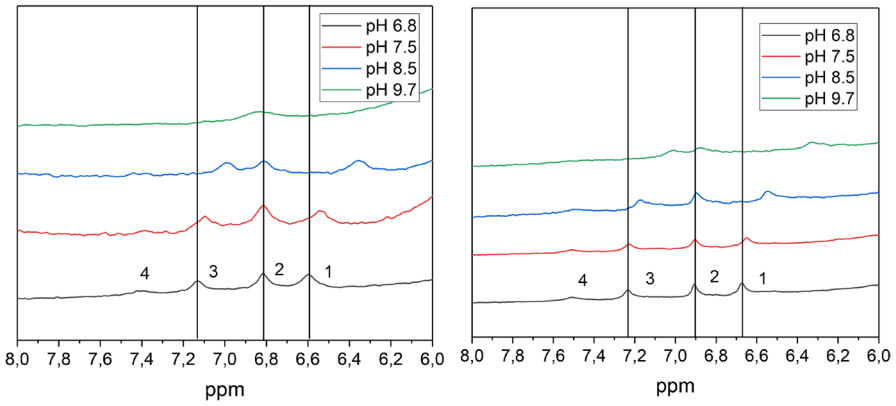

Fig. 6 Fragments of ^{1}H NMR spectra of POPC + emodin suspension (left) and POPC + LA + emodin suspension (right). Numbers corresponds to protons from Fig. 1. NMR assignment was taken from [24]

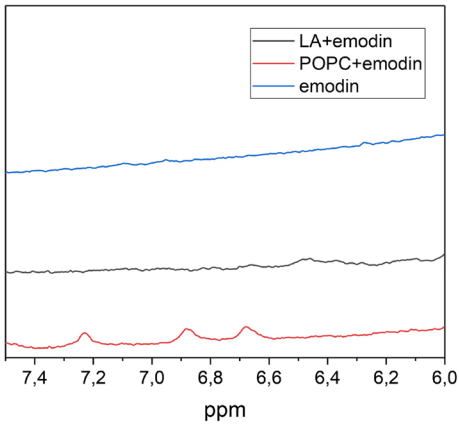

Fig. 7 Fragments of ^{1}H NMR spectra of emodin, POPC + emodin and LA + emodin. Emodin concentration in all samples was 1 mM

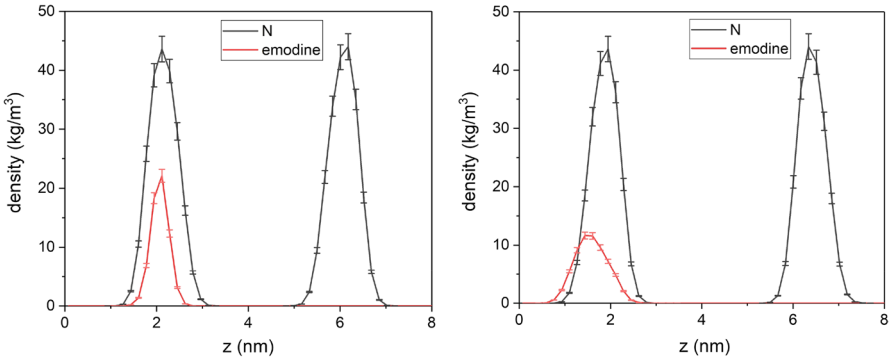

Fig. 8 Density profiles for N atoms of POPC and emodin, POPC + emodin (left) and POPC + LA + emodin (right)

We have also calculated density profiles of hydrogen atoms of emodin OH-groups to understand differences of changes of the chemical shift observed in NMR experiments (Fig. 9). The maximum of density of (*)-hydrogen, which corresponds to the position where the first deprotonation takes place, is the closest to the surface of the POPC bilayer, and the maximum of density of (***)-hydrogen, where the last deprotonation takes place, is the closest to the center of bilayer. The closeness of (*) OH-group to the surface and, correspondingly, to water molecules, could explain the fact that this group deprotonates first.

Also, distances between hydrogen atoms of OH-groups of emodin and the OH-group of LA were measured. Figure 10 demonstrates the time dependence of the distance between (*) OH-group of emodin and the OH group of LA in 100 ns run. The time dependence has several minima, with distances 0.5–0.7 nm and different duration. It means that emodin interacts with LA inside POPC bilayer, and this non-covalent interaction of emodin OH-groups with LA probably prevents dissociation.

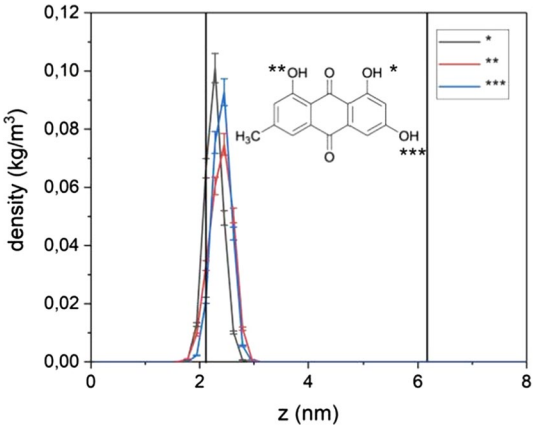

Fig. 9 Density profiles for hydrogens of emodin OH-groups in POPC bilayer without LA. (*), (**) and (***) corresponds to marked hydrogen atoms. Vertical lines corresponds to the maxima of density of POPC nitrogen atoms

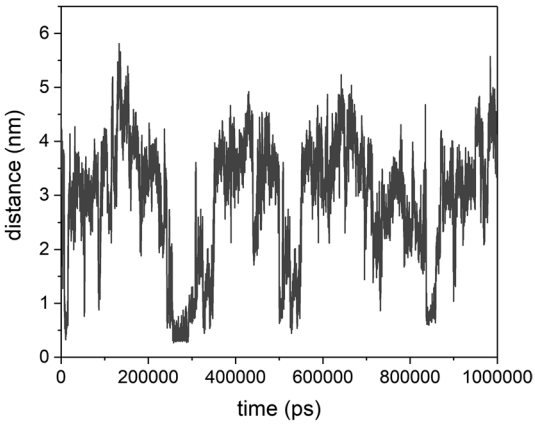

Fig. 10 Distance between (*) OH-group of emodin and OH group of LA

4 Conclusion

In this paper we studied the effect of linoleic acid on the interaction of an emodin molecule with a lipid bilayer by NMR, optical absorption spectroscopy, and molecular dynamics simulations. It was found that in the presence of linoleic acid, the value of the emodin pKa significantly increases. Molecular dynamics simulations show that these changes can be associated with the interaction of emodin and linoleic acid inside the bilayer. Also, it was shown that the order of deprotonation positions in the POPC bilayer differs from the deprotonation order in aqueous solution. It could be connected with the localization of OH-groups in the membrane.

The interaction of emodin with phospholipid bilayer, especially containing unsaturated phospholipids and fatty acids, is important from the point of emodin oxidation activity. It is known, that anthraquinones, in particular, emodin are photosensitizers which produce reactive oxygen species (ROS) during photo excitation [25, 26]. Lipid peroxidation caused by ROS generation could result in cell

destruction. This mechanism of emodin action is prospective for photodynamic therapy of cancer [27].

Acknowledgements The reported study was funded by Russian Ministry of Science and Education (Projects No. 0304-2017-0009 and 0301-2019-0005).

References

1. M. Lucio, J.L. Lima, S. Reis, Curr. Med. Chem. **17**, 1795–1809 (2010). https://www.eurekaselect.com/60389/article. Accessed 26 Apr 2020
2. X. Dong, J. Fu, X. Yin, S. Cao, X. Li, L. Lin, J. Ni, Phytother. Res. **30**, 1207–1218 (2016). https://doi.org/10.1002/ptr.5631
3. D. Shrimali, M.K. Shanmugam, A.P. Kumar, J. Zhang, B.K.H. Tan, K.S. Ahn, G. Sethi, Cancer Lett. **341**, 139–149 (2013). https://doi.org/10.1016/j.canlet.2013.08.023
4. S. Rahimipour, G. Gescheidt, I. Bilkis, M. Fridkin, L. Weiner, Appl. Magn. Reson. **37**, 629–648 (2010). https://doi.org/10.1007/s00723-009-0099-y
5. A.R. da Cunha, E.L. Duarte, H. Stassen, M.T. Lamy, K. Coutinho, Biophys. Rev. **9**, 729–745 (2017). https://doi.org/10.1007/s12551-017-0323-1
6. D.S. Alves, L. Pérez-Fons, A. Estepa, V. Micol, Biochem. Pharmacol. **68**, 549–561 (2004). https://doi.org/10.1016/j.bcp.2004.04.012
7. X. Yang, W. Sheng, G.Y. Sun, J.C.-M. Lee, Neurochem. Int. **58**, 321–329 (2011). https://doi.org/10.1016/j.neuint.2010.12.004
8. L. Kumar, S. Verma, S. Kumar, D.N. Prasad, A.K. Jain, Artif. Cells Nanomed. Biotechnol. **45**, 251–260 (2017).https://doi.org/10.3109/21691401.2016.1146729
9. Y. Wang, L. Jiang, Q. Shen, J. Shen, Y. Han, H. Zhang, RSC Adv. **7**, 41561–41572 (2017). https://doi.org/10.1039/C7RA06088B
10. M. Ibarguren, D.J. López, P.V. Escribá, Biochim. Biophys. Acta BBA—Biomembr. **2014**, 1518–1528 (1838). https://doi.org/10.1016/j.bbamem.2013.12.021
11. X. Lu, G. He, H. Yu, Q. Ma, S. Shen, U.N. Das, J. Zhejiang Univ. Sci. B. **11**, 923–930 (2010). https://doi.org/10.1631/jzus.B1000125
12. H.L. Kantor, J.H. Prestegard, Biochemistry **14**, 1790–1795 (1975). https://doi.org/10.1021/bi00679a035
13. M.J. Abraham, T. Murtola, R. Schulz, S. Páll, J.C. Smith, B. Hess, E. Lindahl, SoftwareX. **1–2**, 19–25 (2015). https://doi.org/10.1016/J.SOFTX.2015.06.001
14. O. Berger, O. Edholm, F. Jähnig, Biophys. J. **72**, 2002–2013 (1997). https://doi.org/10.1016/S0006-3495(97)78845-3
15. K.B. Koziara, M. Stroet, A.K. Malde, A.E. Mark, J. Comput. Aided Mol. Des. **28**, 221–233 (2014). https://doi.org/10.1007/s10822-014-9713-7
16. A.K. Malde, L. Zuo, M. Breeze, M. Stroet, D. Poger, P.C. Nair, C. Oostenbrink, A.E. Mark, J. Chem. Theory Comput. **7**, 4026–4037 (2011). https://doi.org/10.1021/ct200196m
17. M. Stroet, B. Caron, K.M. Visscher, D.P. Geerke, A.K. Malde, A.E. Mark, J. Chem. Theory Comput. **14**, 5834–5845 (2018). https://doi.org/10.1021/acs.jctc.8b00768
18. H.J.C. Berendsen, J.P.M. Postma, W.F. van Gunsteren, J. Hermans, *Interaction Models for Water in Relation to Protein Hydration* (Springer, Dordrecht,1981), pp. 331–342. https://doi.org/10.1007/978-94-015-7658-1_21.
19. M.G. Wolf, M. Hoefling, C. Aponte-Santamaría, H. Grubmüller, G. Groenhof, J. Comput. Chem. **31**, 2169–2174 (2010). https://doi.org/10.1002/jcc.21507
20. B. Hess, H. Bekker, H.J.C. Berendsen, J.G.E.M. Fraaije, J. Comput. Chem. **18**, 1463–1472 (1997). https://doi.org/10.1002/(SICI)1096-987X(199709)18:12<1463:AID-JCC4>3.0.CO;2-H
21. U. Essmann, L. Perera, M.L. Berkowitz, T. Darden, H. Lee, L.G. Pedersen, J. Chem. Phys. **103**, 8577–8593 (1995). https://doi.org/10.1063/1.470117
22. W.G. Hoover, Phys. Rev. A. **31**, 1695–1697 (1985). https://doi.org/10.1103/PhysRevA.31.1695
23. M. Parrinello, A. Rahman, J. Appl. Phys. **52**, 7182–7190 (1981). https://doi.org/10.1063/1.328693

24. K. Danielsen, D.W. Aksnes, G.W. Francis, Magn. Reson. Chem. **30**, 359–360 (1992). https://doi.org/10.1002/mrc.1260300414
25. I. Bilkis, I. Silman, L. Weiner, Curr. Med. Chem. **25**, 5528–5539 (2018). https://doi.org/10.2174/0929867325666180104153848
26. V. Lev-Goldman, B. Mester, N. Ben-Aroya, Y. Koch, L. Weiner, M. Fridkin, Bioconjug. Chem. **17**, 1008–1016 (2006). https://doi.org/10.1021/bc050293r
27. B. Siewert, H. Stuppner, Phytomedicine **60**, 152985 (2019). https://doi.org/10.1016/j.phymed.2019.152985